Effect of model selection on prediction of periodic behavior in gene regulatory networks

Tomáš Gedeon
Department of Mathematics, Montana State University
Bozeman, MT 59715,
Graham Cummins
Department of Mathematics, Washington State University,
and
Jeffrey J. Heys
Chemical and Biological Engineering Department, Montana State University
Bozeman, MT 59715

April 30, 2012

Abstract

One of the the current challenge for cell biology is understanding of the system level cellular behavior from the knowledge of a network of the individual sub-cellular agents. We address a question of how the model selection affects the predicted dynamic behavior of a gene network. In particular, for a fixed network structure, we compare protein-only models with models in which each transcriptional activation is represented both by mRNA and protein concentrations. We compare linear behavior near equilibria for both cyclic feedback systems and a general system. We show that, in general, explicit inclusion of the mRNA in the model weakens the stability of equilibria. We also study numerically dynamics of a particular gene network and show significant differences in global dynamics between the two types of models.

Key words: Gene regulation, model selection.

1 Introduction

As the first decade of the post-genomic era draws to a close, many potential benefits of the human genome project for the medical field are yet to be realized. Knowledge of the elementary building blocks (genes) is necessary, but not sufficient, for understanding the function of cells. Additionally, it is necessary to integrate the qualitative knowledge of gene interaction into a set of workable predictions of cell function. This is a complex task, and a key role is being played by mathematical and computational modeling.

Experimental observations of gene regulation are often represented by a graph of interactions that describe whether a particular transcription factor up- or down- regulates a target gene. While this qualitative information is common, quantitative measurements of essential parameters like binding strengths, transcription and translation rates, and decay rates are harder to come by. Unlike mathematical models in classical physics, where the models express a particular physical law and the parameters have clear physical meaning and are measurable, the models in biology are always an approximation of a more complex, hidden, physical and chemical reality. Under these conditions, conclusions of any biological model can be trusted only if the same conclusions can be drawn from multiple models that are compatible with the available data.

In this situation, model selection is a crucial issue in constructing a model of a gene regulation network. The first choice is the type of the model. Is it reasonable to consider a stochastic model of some system behavior, or alternately a deterministic model, which explicitly tracks chemical concentrations? Deterministic models may also include the spatial, as well as temporal variation of concentrations. In this paper, we consider a deterministic model without spatial dependence; particularly a system of ordinary differential equations modeling the time evolution of chemical concentrations. We then investigate the next choice facing a modeler: Which chemical species are to be included in the model?

In general, the network of relevant interactions includes both proteins and signaling molecules. The interactions in the network may include protein-protein interactions, post-translational modifications like phosphorylation and methylation, and transcriptional regulation, in which a protein up-regulates production of the mRNA for another protein. We consider networks in which transcriptional regulation is the dominant interaction. In such a case, should we model both concentrations of protein and mRNA, or is it sufficient to model the concentrations of the proteins? Both strategies are in use. For example, some models of somitogenesis, where oscillation of gene expression plays a key role, use only protein concentration ([2]) and others use both protein and mRNA concentrations ([11, 16]). A common argument for choosing only the protein concentrations is that mRNA decay rates are typically an order of magnitude larger than those of the proteins and therefore the time evolution of the mRNA may not be important. The goal of this paper is to critically examine this argument in several contexts.

We first analyze loss of stability of an equilibrium via a Hopf bifurcation in negative cyclic feedback systems, which are a class of systems that often arise in models of biochemical oscillations ([9, 3]). We show that the addition of mRNA to such a protein network model can destabilize the equilibrium.

Next we generalize this observation to equilibria of a more general protein network. We consider a model with a single decay rate for all proteins, a single decay rate for all mRNAs, and a single rate of protein production. The nonlinear functions that specify production of mRNA, based on promoter dynamics, are arbitrary. We find that there is always a subset of complex numbers with negative real part, such that if an eigenvalue of a protein-only network lies in this area, a corresponding eigenvalue of the model, that also includes mRNA, has positive real part. This shows that the inclusion of the mRNA may, in general, destabilize an equilibrium. Interestingly, equilibria with real eigenvalues are more difficult to destabilize than with eigenvalues with imaginary parts.

Additionally, if the protein production rate is smaller than the mRNA production rate,

there exists another, smaller, region of complex numbers with positive real part, such that if an eigenvalue of the protein-only model lies here, the corresponding eigenvalues of the mRNA model have negative real part. Under these unlikely conditions, adding mRNA may have a stabilizing effect.

Finally, we numerically analyze the global dynamics of a recent model by Yang *et.al.* [25]. This model has been used to analyze correspondence between a cyclic feedback oscillator (the *repressilator*) and a relaxation type oscillator. Yang's model considers only concentrations of proteins and a signaling molecule. We compare it to an equivalent model that includes mRNA concentrations as well. We show that the bifurcation diagram for the protein only network is qualitatively different from the bifurcation diagram for for the model including mRNA, and the amplitude profile of oscillations is quantitatively different. Using singular perturbation theory we study this system in two limits; when protein turnover is much faster that that of mRNA and when the mRNA turnover is much faster than that of protein. In both cases there is a slow manifold in the combined model with its slow dynamics mimicking the dynamics of the protein only network. However, when the mRNA turnover is about ten times faster than the protein turnover, which is the biologically realistic ratio, there are significant differences in both local and global dynamics between the protein only model and the model that also includes mRNA. These results illustrate the main message in this paper; that conclusions drawn from a network model should be used with caution, and with an understanding that reasonable changes in the model may lead to different conclusions.

Our work only starts an exploration of the effect of model selection on model-based predictions of the dynamics of gene regulation systems. We hope our results will contribute to a more complete theory that can guide modelers in this fast developing area of mathematical biology.

2 Basic model

We will ask the general question whether, and to what extent, the dynamics of a gene regulatory network model considering only protein concentrations are the same as those of an extended model including both mRNA and protein concentrations. For simplicity we assume that the production of the proteins from mRNA follows a linear ODE [3, 4], and all the interactions between proteins are mediated through interaction on the gene promoters. In particular, we want to compare the dynamics of

$$\begin{aligned} \dot{x}_1 &= f_1(x_1, \ldots, x_n) - d_1 x_1 \\ \vdots &\quad \vdots \\ \dot{x}_n &= f(x_1, \ldots, x_n) - d_n x_n \end{aligned} \tag{1}$$

with the dynamics of a more complicated model

$$\begin{aligned} \dot{x}_1 &= c_1 y_1 - d_1 x_1 \\ \dot{y}_1 &= f_1(x_1, \ldots, x_n) - b_1 y_1 \\ \vdots & \quad \vdots \\ \dot{x}_n &= c_n y_n - d_n x_n \\ \dot{y}_n &= f(x_1, \ldots, x_n) - b_n y_n. \end{aligned} \tag{2}$$

The variables x_i represent concentration of the i-th protein and y_i the concentrations of the i-th mRNA. The nonlinearities f_i are typically Hill type rational functions, and may be the result of a more complex model of promoter occupancy ([21, 7, 8]).

We first note that the equilibria of (1) satisfy

$$f_i(x_1, \ldots, x_n) = d_i x_i \text{ for all } i$$

while equilibria of (2) satisfy

$$f_i(x_1, \ldots, x_n) = \frac{b_i}{c_i} d_i x_i \text{ for all } i. \tag{3}$$

Since the functions f_i are typically sigmoidal, even this small change can lead to different numbers of equilibria in the system. However, we note that

Lemma 2.1 *1. If $b_i = c_i$ for all i then $(x_1, \ldots, x_n)$ is an equilibrium of (1) if, and only if, $(x_1, x_1, x_2, x_2, \ldots, x_n, x_n)$ is an equilibrium of the system (2).*

2. If $(0, 0, \ldots, 0)$ is an equilibrium of (1) then it is also an equilibrium of (2), for any values of b_i and c_i.

In particular, an assumption of a much faster turnover of mRNA, modeled by assuming $c_i = d_i = \epsilon$, does not automatically lead to comparable equilibria in (1) and (2).

We will show that even when the equilibria are comparable, their stability can change dramatically when the model changes from (1) to (2).

3 Results

3.1 A simple feedback loop

As a first example we study a class of models called *cyclic feedback systems*. An early synthetic biology construct that produces oscillations in live cells, known as the *repressilator* [3], can be modeled as a negative cyclic feedback system. In the repressilator construct, three transcriptional regulators A,B and C each repress expression of a the next regulator: A represses B, B represses C and C represses A. Ellowitz and Leibler [3] and later Garcia-Ojalvo *et. al.* [4] chose to model the repressilator using both the concentrations of proteins (A,B,C) and the concentrations of the corresponding mRNAs (a,b,c). A model that considers only protein concentrations is also possible, of course ([25]).

A cyclic feedback system has the form

$$\begin{aligned} \dot{x}_1 &= \delta a_1 f_1(x_n) - d_1 x_1, \\ \dot{x}_i &= a_i f_i(x_{i-1}) - d_i x_i,\ i = 2, \ldots, n \end{aligned} \tag{4}$$

where $d_i > 0, a_i > 0$ for all $i = 1, \ldots, n$. In biological models where the variables denote non-negative concentrations, the functions f_i usually include constant terms, which model background expression of the given protein. Thus the system admits a non-negative equilibrium. To simplify our discussion we shift the variables in such a way that one of this equilibria is at the origin. In the new coordinates we assume that the functions f_i satisfy either

$$\frac{df_i}{dx_{i-1}}(x_{i-1}) > 0 \text{ for all } x_{i-1} \tag{5}$$

or a weaker condition

$$x_{i-1} f_i(x_{i-1}) > 0 \text{ for all } x_{i-1} \neq 0. \tag{6}$$

In the second case we call the system a *cyclic feedback system*; in the first case a *monotone cyclic feedback system.* We can also assume without loss that $\frac{df_i}{dx_{i-1}}(0) = 1$, since a_i are arbitrary.

The constant $\delta = \pm 1$ determines whether the system is *positive* or a *negative* cyclic feedback system. We note that a more general system where in each equation we can chose a sign of the interaction δ_i, can be put into the form (4) by a simple change of variables [12, 5]. Then the overall feedback sign $\delta = \delta_1 \delta_2 \ldots \delta_n$ is a product of the individual signs. In particular, the repressilator is a negative feedback system since the overall feedback is a product of 3 negative feedbacks $A \to b, B \to c$ and $C \to a$, representing regulation of mRNA; and 3 positive feedbacks $a \to A, b \to B$ and $c \to C$, representing protein production from mRNA. Observe that if we chose to model only protein concentrations in the repressilators, there would be 3 negative feedbacks $A \to B, B \to C$ and $C \to A$, again resulting in a negative feedback. Note that the origin is a unique equilibrium in the negative monotone cyclic feedback system [5].

The variables x_i in (4) describe concentrations of proteins. We now introduce the enlarged system where for each species we also consider the concentration of mRNA.

$$\begin{aligned} \dot{y}_1 &= -b_1 y_1 + \delta a_1 f_1(x_n) \\ \dot{x}_1 &= -d_1 x_1 + c_1 y_1 \\ \dot{y}_i &= -b_i y_i + a_i f_i(x_{i-1}) \qquad i = 2, \ldots, n \\ \dot{x}_i &= -d_i x_i + c_i y_i, \qquad i = 2, \ldots, n. \end{aligned} \tag{7}$$

We see that the basic cyclic structure of the feedback system has not changed and, as in the repressilator example, the sign of the feedback remains the same.

The dynamics of cyclic feedback systems are known in great detail [13, 5, 6, 14]. Here we discuss a Hopf bifurcation, which is relevant to emergence of oscillations in biological systems. The linearization of the system (4) has the form

$$\dot{x} = (A - D)x$$

where $D = diag(d_1, \ldots, d_n)$ and A is a matrix where the entries $a_i, i = 2, \ldots, n$ lie in the matrix position $(i, i-1)$, and a_1 in the position $(1, n)$. The linearization of the system (7) is a linear system

$$\dot{z} = (W - Q)z$$

where $z = (x_1, y_1, \ldots, x_n, y_n)$ is a combination of vectors x and y, $Q = diag(b_1, d_1, b_2, d_2, \ldots, b_n, d_n)$ and non-zero entries c_i, a_i lie in the same off-diagonal pattern in matrix W, as the pattern formed by entries a_i in the matrix A.

A following sufficient condition for stability of equilibria was proved in [24, 23], see also ([5, 1, 22]).

Theorem 3.1 *All eigenvalues of the matrix $A - D$ have negative real part, if*

$$\frac{a_1 a_2 \ldots, a_n}{d_1 d_2 \ldots d_n} < \frac{1}{\cos(\pi/n)^n}. \tag{8}$$

This condition is necessary, when $d_1 = d_2 = \ldots d_n$.

Corollary 3.2 *Assume $\frac{c_1,\ldots,c_n}{b_1,\ldots,b_n} \geq 1$. Then if the equilibrium $(0, \ldots, 0)$ is stable in (7), then it is stable in (4). The opposite implication is not true.*

Proof. The condition equivalent to (8) for the larger system (7) reads

$$\frac{a_1 a_2 \ldots, a_n c_1 \ldots c_n}{d_1 d_2 \ldots d_n, b_1, \ldots, b_n} < \frac{1}{\cos(\pi/2n)^{2n}}.$$

If $\frac{c_1,\ldots,c_n}{b_1,\ldots,b_n} \geq 1$ then we have an estimate

$$\frac{a_1 a_2 \ldots, a_n}{d_1 d_2 \ldots d_n} \leq \frac{a_1 a_2 \ldots, a_n c_1 \ldots c_n}{d_1 d_2 \ldots d_n, b_1, \ldots, b_n} < \frac{1}{\cos(\pi/2n)^{2n}} < \frac{1}{\cos(\pi/n)^n},$$

which verifies the secant condition for (4). The second part of the proof follows from the fact that the condition (8) is sharp, when the diagonal matrix is a multiple of the identity. □

Therefore the equilibrium stability condition for the larger system (7) is more restrictive than the stability condition for the simpler system (4). Note that the assumption of the corollary is satisfied, for the negative cyclic feedback system, if the protein production rate c_i is greater or equal to the mRNA decay rate b_i. We conclude that in this case the addition of mRNA into the model makes the equilibrium less stable.

3.2 Stability of equilibria in a general system

In this section we address the relationship between the stability of equilibria in the more general systems (1) and (2). Linearization of (1) at an equilibrium E has the form

$$\dot{x} = Ax - Dx \tag{9}$$

where $D = diag(d_1, \ldots, d_n)$ and

$$A = \frac{df}{dx}|_E \tag{10}$$

is the linearization of f at an equilibrium E. Changing system (1) to the larger system (2) changes, in general, the equilibrium E to a different equilibrium $\bar{E}$. The linearization of (2) at $\bar{E}$ is

$$\begin{aligned} \dot{x} &= Cy - Dx \\ \dot{y} &= \bar{A}x - By, \end{aligned} \tag{11}$$

where $B = diag(b_1, \ldots, b_n), C = diag(c_1, \ldots, c_n)$ and

$$\bar{A} = \frac{df}{dx}|_{\bar{E}}.$$

The relationship between E and $\bar{E}$, and therefore A and $\bar{A}$, depends on the details of the system. However, under conditions specified in Lemma 2.1 we have $A = \bar{A}$ and we can compare stability of the corresponding equilibria in (1) and (2). To do so we relate each eigenvalue z of the problem (9) to a pair of eigenvalues $\lambda^{\pm}$ of the problem (11).

Theorem 3.3 *Consider linear systems (9) and (11) with $A = \bar{A}$. Assume that $d_i = d > 0, b_i = b > 0$ and $c_i = c > 0$ for all i. Then there is an open unbounded region U of complex numbers with negative real part, such that if an eigenvalue z of (9) lies in U, then there is a corresponding pair of eigenvalues of (11) $\lambda^{\pm}$ such that λ^- has negative and λ^+ has a positive real part (see Figure 1). In addition,*

1. *When $\frac{c}{b} > 1$, the set U meets the real axis in a non-empty set*

$$U \cap \Re e = \{x + iy \mid x \in ((\frac{b}{c} - 1)d, 0), y = 0\}.$$

2. *if $\frac{c}{b} = 1$, then*

$$\mathrm{cl}(U) \cap \Re e = \{0\}.$$

3. *If $\frac{c}{b} < 1$ then there is another, bounded region V of complex numbers with positive real part, such that if an eigenvalue z of (9) lies in V, then both corresponding eigenvalues of (11) $\lambda^{\pm}$ have negative real parts. Furtermore,*

$$V \cap \Re e = \{x + iy \mid x \in (0, (\frac{b}{c} - 1)d), y = 0\}.$$

The existence of the set U generalizes the result from the cyclic feedback system in Corollary 3.2: the addition of mRNA can destabilize equilibria in the model. We note that in the case when $b = c$ only non-real eigenvalues z lie in U. This means that when $b = c$ and an equilibrium has only real eigenvalues, its stability in (9) and (11) is the same. This clearly does not imply that the *number* of eigenvalues with positive or negative real part are the same, since the models have different dimensionality.

When $c < b$ there is an additional small region V in the positive half of the complex plane, such that when an eigenvalue z of (9) lies in this region, then the addition of mRNA has a stabilizing effect.

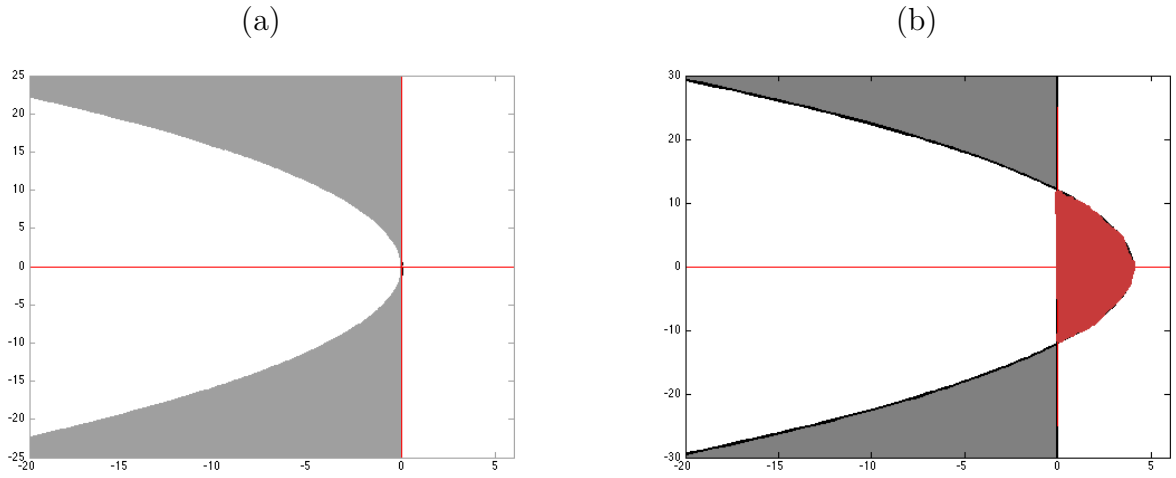

Figure 1: (a) Region U for $b = c = 1$ and $d = 4$ (dark). If an eigenvalue of the problem (9) is in U, then one of the corresponding eigenvalues λ^+ of the problem (11) has a positive real part. Region V is empty. (B) Region U (grey) and a region V (red) for $b = 2$, $c = 1$ and $d = 4$. The region V is bounded and intersects the real axis, while the region U is unbounded and does not.

3.2.1 Singular limit

In this section we consider a singular limit where the protein turnover is much slower than that of the mRNA. Note that this assumption implies that both the production and the decay of proteins is slower than production and decay of mRNA. Since the lifetime of mRNA's is on the order of minutes and and the lifetime of proteins can be on the order of hours, the assumption that the decay rate of proteins is much lower that that of mRNA is justified. However the rates of production of mRNA and proteins are much closer together, since they are linked by the process of translation.

The usual way that the faster turnover of mRNA is modeled is to introduce a small parameter ϵ that multiplies both the protein production and decay terms.

$$\begin{aligned} \dot{x} &= \epsilon(Cy - Dx) \\ \dot{y} &= Ax - By. \end{aligned} \tag{12}$$

We replace $c \to \epsilon c$ and $d \to \epsilon d$ in the analysis above. In particular we see that the boundary of the region $W_1 = W_1(\epsilon)$ is formed by the line ϵd and thus it converges to the imaginary axis as $\epsilon \to 0$. The bound (26) on the set $Y = Y(\epsilon)$ takes the form

$$u > 2\frac{(b + \epsilon d)^2}{(1 + \cos\theta)}$$

while the set is $X(\epsilon) = Y(\epsilon) - (\epsilon d - b)^2$. Note that the set $X(\epsilon)$ does have a limiting parabolic shape $X(0) = Y(0) - b^2$ which has an apex at $(0, 0)$ and $Y(0)$ is given by $u > 2\frac{b^2}{(1+\cos\theta)}$. However, since $Re^{i\phi} \in X$ if, and only if, $4c\epsilon re^{i\phi} \in W_2$, the lower bound that defines W_2 goes to ∞ along any ray, $\theta = \text{const}$. This not only shows that in the limit $\epsilon \to 0$ we recover the

stability of the system (9), but also that for each fixed $\epsilon \neq 0$ there is an unbounded region $U(\epsilon)$ in the complex plane where the stability under (9) does not agree with stability under (11).

Finally, when $b \neq c$ as in (12), the linearization (9) of the problem (1) occurs at a potentially different equilibrium than the linearization (11) of the problem (2). Our analysis in the previous paragraph does not address this issue.

3.3 Analysis of a genetic oscillator

In the previous sections we concentrated on the stability of the equilibria and a Hopf bifurcation. In this section we will consider the global oscillatory dynamics of a gene network.

In a recent paper [25] the authors analyze a simple network of three molecular species. Their model is motivated by the desire to study two mechanisms that were identified previously in conjunction with models of periodic behavior. The negative cyclic feedback we considered in the section 3.1 can generate oscillations in live cells [3]. An apparently different mechanism is driving the cell cycle in early embrios [17, 18, 19, 20]. This mechanism is characterized by abrupt transitions, and includes processes occurring on multiple timescales, reminiscent of a *relaxation oscillator*. Although these mechanisms are not mutually exclusive, several articles ([4, 10, 15]) have attempted to characterize phenomena as being modeled by one or the other limit, and have drawn contrasts between them in terms of their response to noise, and the synchronization behavior of groups of them. In [25] the authors studied a three species model that is capable of simulating the behavior of both a repressilator and a relaxation oscillator at different parameter values, and can also show intermediate behaviors. Their system is described by:

$$\begin{aligned} \dot{x}_1 &= \frac{\alpha_1}{1+x_2^n} - x_1 \\ \dot{x}_2 &= \frac{\alpha_1}{1+x_3^n} + \frac{\alpha_2}{1+x_1^n} - x_2 \\ \dot{x}_3 &= \epsilon(\frac{\alpha_1}{1+x_1^n} - x_3) \end{aligned} \tag{13}$$

When $\alpha_2 << 1$ and $\epsilon = O(1)$ the system models the cyclic feedback system (repressilator), while when $\alpha_2 = O(1)$ and $\epsilon << 1$, the system exhibits relaxation oscillations.

Yang *et.al* [25] provide a detailed bifurcation analysis of this oscillator as a function of parameters α_2 and ϵ, when $n = 3, \alpha_1 = 5$. In Figure 2.a we show the region in this parameter space where the system (13) exhibits stable oscillations. The upper and lower boundaries are curves of Hopf bifurcations, while the vertical part of the boundary is a saddle-node bifurcation on a periodic orbit (SNIC). The two dashed lines on the right are saddle node bifurcations of equilibria. The model exhibits three equilibria between these lines and one equllibrium outside of these lines. The boundary piece connecting the upper Hopf curve to the SNIC curve is a locus of homoclinic bifurcations. For more details on the analysis the reader is referred to the original paper.

In the model of Yang *et.al* [25] the first two equations represent protein concentrations while the third represents a soluble small molecule. With this in mind we would like to compare the dynamics of (13) to a system where we replace each of the first two equations

with a pair of equations that model both mRNA and protein concentrations. Our model has the form:

$$\begin{aligned}
\dot{y}_1 &= \frac{\alpha_1}{1+x_2^n} - b_1 y_1 \\
\dot{x}_1 &= c_1 y_1 - d_1 x_1 \\
\dot{y}_2 &= \frac{\alpha_1}{1+x_3^n} + \frac{\alpha_2}{1+x_1^n} - b_2 y_2 \\
\dot{x}_2 &= c_2 y_2 - d_2 x_2 \\
\dot{x}_3 &= \epsilon(\frac{\alpha_1}{1+x_1^n} - x_3).
\end{aligned} \tag{14}$$

The variables y_1 and y_2 represent concentrations of mRNA, and x_1, x_2 concentrations of the same proteins as in (13). Since we would like to compare this model to (13), we would like to ensure that it has the "same" equilibria, in the sense of Lemma 2.1. Therefore we choose the mRNA decay rates $b_1 = b_2 = 1$, and set all the protein production rates c_i equal to the decay rates d_i. Additionally, we select $n = 3, \alpha_1 = 5$, to match choices in [25].

A principal argument against needing to explicitly model mRNA dynamics in this way is the different characteristic time scale of mRNA compared to protien processes. Consequently, we are interested in investigating the effects of using different timescales for these components. To facilitate this investigation, we add rate parameters R_p, R_m, which scale the rates of protein, and mRNA processes respectively. This, combined with the constraints on the constants b, c, d, n, α_1, results in the model:

$$\begin{aligned}
\dot{y}_1 &= R_m(\frac{5}{1+x_2^3} - y_1) \\
\dot{x}_1 &= R_p(y_1 - x_1) \\
\dot{y}_2 &= R_m(\frac{5}{1+x_3^3} + \frac{\alpha_2}{1+x_1^3} - y_2) \\
\dot{x}_2 &= R_p(y_2 - x_2) \\
\dot{x}_3 &= \epsilon(\frac{5}{1+x_1^3} - x_3)
\end{aligned} \tag{15}$$

This choice of parameters is somewhat redundant, since we would only need a single rate scaling parameter to change the relative rates of mRNA and protein processes, but the use of an extra parameter simplifies the model conceptually. We note that the parameter ϵ changes the system dynamics by changing the ratio of large molecule rates $(\dot{x}_1, \dot{x}_2)$ to the the small molecule rate $\dot{x}_3$. When we model the large molecule processes with separate mRNA and protein steps, the overall rate of this component is determined by the slower of these two processes. Consequently, when we vary R_p and R_m the effect of ϵ on system dynamics is scaled by $\min(R_p, R_m)$. Using two explicit parameters, as we do here, allows us to vary the relative rates of protein and mRNA steps, while maintaining a constant rate of the whole large molecule component, by constraining $\min(R_p, R_m) = 1$. This constraint renders absolute values of ϵ comparable between different tested conditions. This also applies to comparisons that depend on absolute time, such as oscillation frequency.

Beginning with the case where protein and mRNA components have similar rates, $R_p = R_m = 1$, we compare a bifurcation diagram in parameters α_2 and ϵ of model (13) to the same diagram for (15). The results are shown in Figure 2.a and b respectively. While the boundaries of the diagrams in Figures 2.a and 2.b have some similarities, there are important quantitative and qualitative differences. The most striking qualitative difference is that the oscillatory region is bounded in ϵ for small α_2 in the protein only model (Figure 2.a), but seems to be unbounded in model (15) (Figure 2.c). We have observed oscillations all the way to $\epsilon = 1000$ (data shown only to $\epsilon = 3$). The main quantitative differences notable in Figure 2a and b are the position of the lower Hopf bifurcation curve (much lower in Figure 2.b) and lower position of the cusp on the right. Additionally, even where both models show stable oscillations, the amplitudes of these oscillations sometimes differ substantially (see Figure 3.a and b, and the description of this figure in the following section).

3.3.1 Fast protein dynamics

We now analyze the situation when $R_m = 1$ and $R_p >> 1$ in model (15), which corresponds to protein turnover that is much faster than that of mRNA. Although this case is not biologically realistic, we consider it because as $R_p \to \infty$, there is a detailed and well defined correspondence between the global dynamics of (13) and (15). As is clear from the argument below, similar result holds for the more general model (14). Indeed, writing $\zeta = 1/R_p << 1$ (and fixing $R_m = 1$) the system (15) becomes

$$\begin{aligned}
\dot{y}_1 &= \frac{5}{1+x_2^3} - y_1 \\
\zeta \dot{x}_1 &= y_1 - x_1 \\
\dot{y}_2 &= \frac{5}{1+x_3^3} + \frac{\alpha_2}{1+x_1^3} - y_2 \\
\zeta \dot{x}_2 &= y_2 - x_2 \\
\dot{x}_3 &= \epsilon(\frac{5}{1+x_1^3} - x_3).
\end{aligned}$$

Setting $\zeta = 0$ we obtain a 3-dimensional invariant slow manifold in R^5 given by

$$M := \{(y_1, x_1, y_2, x_2, x_3) \mid y_1 = x_1, \quad y_2 = x_2\}$$

on which the dynamics is given precisely by the system (13).

Our numerical simulations confirm this conclusion. With $R_p = 2000$ protein turnover is three orders of magnitude faster than that of mRNA, and protein concentrations are strongly slaved to the mRNA dynamics. In this limit, our model yields the bifurcation diagram shown in Figure 2.c, which is essentially identical to the bifurcation diagram of model (13), shown in Figure 2.a. Additionally, the amplitude profile of oscillations in model (15) with $R_p = 2000$ (shown in Figure 3.a) is visually identical to the corresponding profile of model (13) (this image is not shown). We note that there is a relatively smooth transition from the behavior shown in Figure 2.b to that seen in Figure 2.c as R_p scales from 1 to 2000. Significant differences in the bifurcation structures remain evident for values of R_p up to about 400, and perceptible differences remain up to $R_p \approx 1500$ (data not shown).

In Figure 3 we show the oscillatory regions of (15), including both the bifurcation diagram (as in Figure 2) and also the amplitudes of oscillations within the oscillatory region, measured as described in Section 5.2. This gives a more complete picture of quantitative changes in system behavior. Figure 3.a shows the case $R_p = 2000$, and has visually identical behavior to the protein-only model (13) (we omit the identical plot generated by the simple model, to conserve space). Figure 3.b shows the case of model (15) with $R_p = R_m = 1$. We see that in addition to changes in the region of stable oscillations, even in areas of the parameter space where both models show stable oscillation, the quantitative nature of these oscillations may be quite different. Particularly, for $\alpha_2 \leq 1, \epsilon < .5$, there are several regions where both models oscillate, but the oscillation in the protein-only model has much smaller amplitude than observed in the model that includes mRNA. This region of the parameter space is potentially quite important to biologically realistic relaxation-type oscillators, and thus this quantitative difference may be at least as important to real systems as the changes in the bifurcation structure.

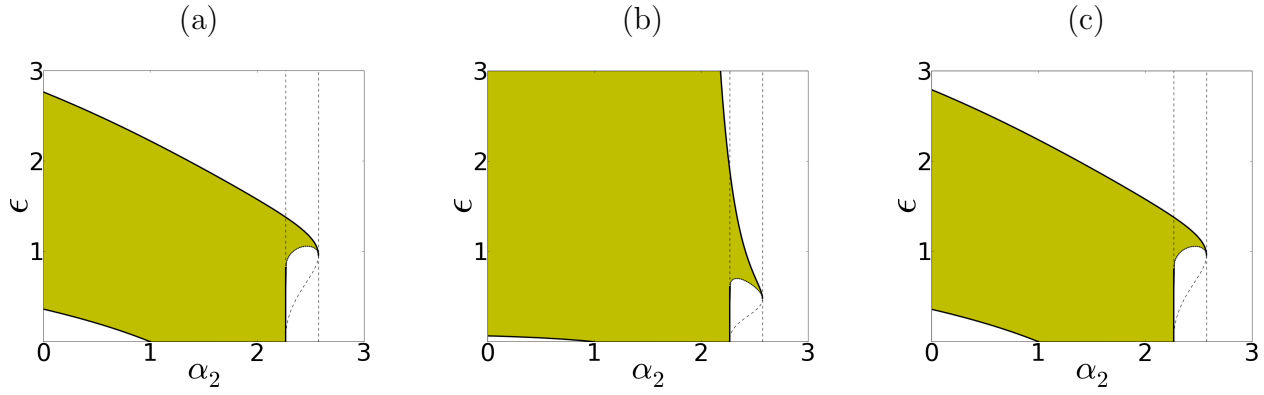

Figure 2: Shaded region in the parameter space exhibits stable oscillations. (a) three dimensional protein only network (13) of Yang *et.al* [25]; (b) Protein and mRNA system (15), with similar protein and mRNA process rates ($R_p = R_m = 1$); (c) protein and mRNA system (15) with very fast protein rates ($R_p = 2000$).

3.3.2 Fast mRNA dynamics

We now consider the more biologically realistic situation when mRNA has faster production and decay rates than the protein. In this case, we fix $R_p = 1$, and increase R_m. To investigate the correspondence between the dynamics of (13) and (15) for large R_m, we set $\delta = 1/R_m$

and then let $\delta = 0$. The system (15) then takes the form

$$\begin{aligned} 0 &= \frac{5}{1+x_2^3} - y_1 \\ \dot{x}_1 &= y_1 - x_1 \\ 0 &= \frac{5}{1+x_3^3} + \frac{\alpha_2}{1+x_1^3} - y_2 \\ \dot{x}_2 &= y_2 - x_2 \\ \dot{x}_3 &= \epsilon(\frac{5}{1+x_1^3} - x_3), \end{aligned}$$

The slow manifold, parameterized by (x_1, x_2, x_3), is a three dimensional manifold in a five dimensional space, given by

$$y_1 = \frac{5}{1+x_2^3}, \quad y_2 = \frac{5}{1+x_3^3} + \frac{\alpha_2}{1+x_1^3}. \tag{16}$$

Substituting (16) into the second, fourth and fifth equations yields *slow dynamics* which are identical to (13). The dynamics of the full system (15) with $R_p = 1$ and $R_m >> 1$ show a rapid relaxation towards this slow manifold.

We conclude that in both limits of fast protein turnover ($R_p >> 1$ and $R_m = 1$) and fast mRNA turnover ($R_p = 1$ and $R_m >> 1$), the dynamics on the slow manifold are the dynamics of (13). However, we now show that for a realistic ratio of protein to mRNA turnover the dynamics differ significantly from those of (13).

Figure 3.c and d show the bifurcation structure and oscillation amplitudes for two cases where $R_p = 1, R_m > 1$. Figure 3.c is the most biologically realistic case, with $R_m = 10$, mRNA dynamics one order of magnitude faster than protein dynamics. Comparing to Figure 3.a ($R_p = 2000$, behavior equivalent to the protein only model), we see significant differences in the position of the upper Hopf curve, which bounds the oscillatory region in the direction of increasing ϵ. There are also substantial quantitative differences in the amplitudes of oscillations at many parameter values within the oscillatory region. Figure 3.d shows the case of mRNA 2000 times faster than proteins. This is a much higher ratio of mRNA to protein rate than is found in most real systems. Here, the differences in the shape of the oscillatory region compared to the simplified model are substantially reduced. Since the boundaries of this region are mostly determined by Hopf bifurcation curves, which are computed from linearization at the set of equilibria, it is not surprising that the outlines of the oscillatory region in Figure 3.d resemble the region in Figure 2.a. Even for this very high ratio of mRNA to protein rates, however, quantitative differences in the oscillation amplitude profile remain, in contrast to the case $R_p = 2000$.

We want to emphasize that in the case of $R_m = 10$, which represents a biologically reasonable assumption that the mRNA turnover is 10 times faster than that of proteins, there are significant changes in the global dynamics of system (15) compared to system (13). The argument that the faster turnover of mRNA validates modeling only protein dynamics is not justified in this case. In the limit of extremely fast mRNA processes, the mRNA and protein only models are still not equivalent, but might be argued to be sufficiently similar to justify the approximation. Biologically realistic separation of protein and mRNA timescales is not nearly sufficient to approach this limit for system (14).

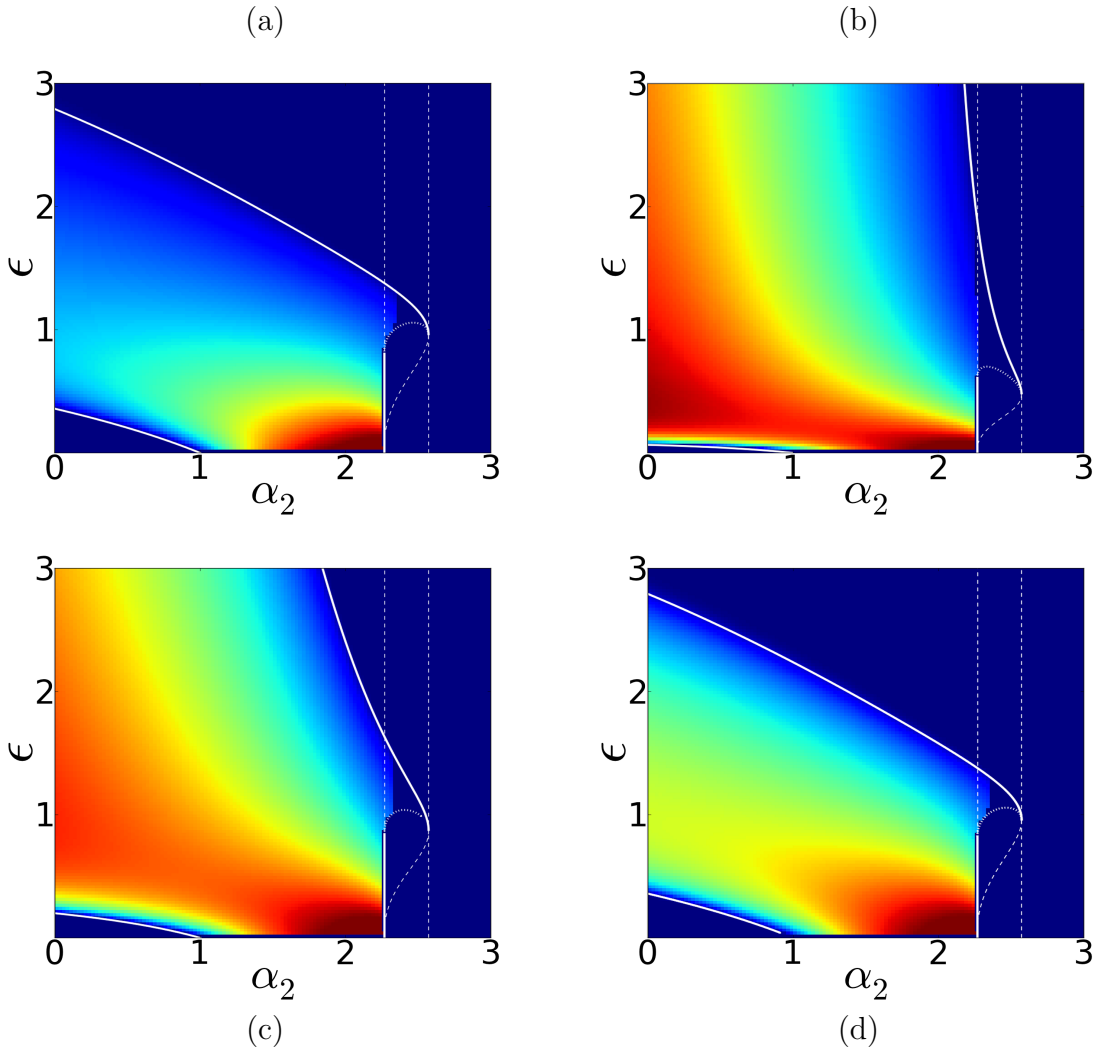

Figure 3: Amplitude of stable oscillations as a function of the parameters. The warmer colors correspond to larger oscillations. The color scale is the same in all figures: the same color corresponds to the same amplitude. (a) system (15) with $R_p = 2000$ recapitulates dynamics of the model (13) of Yang *et. al.* [25]; (b) system (15) with $R_p = R_m = 1$ shows significant differences in oscillation stability and amplitude (c) system (15) with biologically plausible ratio of mRNA to protein turnover rate $R_m = 10$ shows significant differences in dynamics compared to (a) as well; (d) system (15) with very fast mRNA turnover $R_m = 2000$ shows a similar region of stable oscillation to (a), but retains differences in oscillation amplitude, in spite of the fact that the linear approximations at equilibria are similar to those of (13).

We conclude that model selection can significantly change both qualitative and quantitative behavior of gene network models and different, reasonable, choices of models can result in substantially different predictions of behavior. Additionally, in this system we find that even if the timescale of mRNA processes is ten times faster than that of protein processes, including mRNA in the model still changes the model's dynamics, both qualitatively and quantitatively.

4 Discussion

As the use of mathematical models of gene regulation becomes more common, the question of reliability of model predictions is becoming more central. Since many modeling approaches can be realistically used in any situation, the question of how model prediction depends on this choice needs to be addressed.

In this work we analyze one such choice. The structure of the gene networks we consider can be represented in the form of a directed signed graph, where connections represent either up-or down-regulation of the gene corresponding to the target node by the gene corresponding to the source node. This specification leaves many modeling choices still open. In particular, it does not specify if for each gene both protein and mRNA abundances should be modeled, or if only protein abundances would suffice. Both of these model types are routinely used. Leaving aside a (very interesting) question of correspondence between dynamics of a deterministic or a stochastic model, we compare dynamics of two ODE systems, which are both constrained by the same gene network interaction graph with n nodes. The n-dimensional system that uses one variable per vertex of the graph represents a choice of modeling protein abundances, while a 2n-dimensional system which uses two variables per vertex represents a choice to model both mRNA and protein abundances.

We compare the dynamics of these models in three different settings. First we show that, in cyclic feedback systems, the addition of mRNA can only destabilize an equilibrium. Cyclic feedback systems are a class of systems that often arise in models of biochemical oscillations ([9, 3])

We then generalize our analysis to equilibria of a more general protein network. We assume a single decay rate for all proteins, a single decay rate for all mRNAs, and a single rate of protein production, but allow the nonlinear functions that specify production of mRNA, based on promoter dynamics to be arbitrary. We find that there is always a subset of complex numbers with negative real part, such that if an eigenvalue of a protein-only network lies in this area, a corresponding eigenvalue of the model, that also includes mRNA, has positive real part. This shows that the inclusion of the mRNA may, in general, destabilize an equilibrium. In some special circumstances, inclusion of mRNA may also stabilize the equilibrium, but these cases are not biologically plausible.

Finally, we numerically analyze the global dynamics of a recent gene regulation model by Yang *et.al.* [25], which has been used to investigate correspondence between a cyclic feedback oscillator (the *repressilator*) and a relaxation type oscillator. Yang's model considers only concentrations of proteins and a signaling molecule. We compare it to an equivalent model that includes mRNA concentrations as well. We show that the bifurcation diagram for the protein only network is qualitatively different from the bifurcation diagram for for the model including mRNA, and the amplitude profile of oscillations is quantitatively different.

We conclude that, in general, the addition of mRNA concentrations as separate state variables can result in qualitative changes to the dynamics of gene network models. In the specific case of the model from [25], we find significantly altered behavior with the explicit modeling of mRNA. A common argument for simplifying gene regulation models by not explicitly tracking mRNA is that mRNA dynamics are often much faster than protein dynamics. We find that, although in the limit of a very large separation of timescales between the protein and mRNA processes, this is a valid argument, for biologically probable values

of this separation, significant differences remain. Effective models of biological processes will need to include some simplification, given the very large number of possible components to track in a real biological system. We find, however, that a reasonable choice of simplification can result in a model with different behaviors. We thus suggest that caution will be needed when choosing how a model should be simplified.

Our work is only a first step in what we hope will be an important line of research that aims to rigorously compare dynamics of different models, all of which are compatible with a given structural constraint. In our case the structural constraint is the signed graph of interaction between genes or, more generally, species. An obvious next steps would be to include the effect of a transcriptional and translational delay into an ODE model and investigate the dynamics of an ODE model and an ODE model with delays, or compare stochastic and deterministic dynamics with the same structure. While partial results exist in both of these areas, a number of questions remain open.

5 Appendix

5.1 Proof of Theorem 3.3

We start by comparing the roots of the characteristic polynomial of (9)

$$det(A - D - \lambda I) =: \Pi_{i=1}^{n}(\lambda - z_i) \tag{17}$$

with the characteristic polynomial of (11)

$$det\, Q := det \begin{bmatrix} -D - \lambda I & C \\ A & -B - \lambda I \end{bmatrix}. \tag{18}$$

If we multiply the $n+l$ column of Q by $\frac{d_l+\lambda}{c_l}$ and add it to the lth column of Q for $l = 1, \ldots, n$ then the determinant in (18) does not change and we get

$$det\, Q = det \begin{bmatrix} 0 & C \\ A - (B + \lambda I)C^{-1}(D + \lambda I) & -B - \lambda I \end{bmatrix}. \tag{19}$$

Now we multiply the l row of the above matrix by $\frac{b_l+\lambda}{c_l}$ and add it to the $n + l$th row for $l = 1, \ldots, n$. After this operation

$$det\, Q = det \begin{bmatrix} 0 & C \\ A - (B + \lambda I)C^{-1}(D + \lambda I) & 0 \end{bmatrix}.$$

By exchanging the first n and second n rows we finally get

$$\begin{aligned} det\, Q &= (-1)^{n^2} det \begin{bmatrix} A - (B + \lambda I)C^{-1}(D + \lambda I) & 0 \\ 0 & C \end{bmatrix} \\ &= (-1)^{n^2} det\, C\; det\, (A - (B + \lambda I)C^{-1}(D + \lambda I)). \end{aligned} \tag{20}$$

Up to this point our argument is general and allows arbitrary diagonal matrices B, C and D. To make further progress we assume that each of the diagonal matrices is constant.

That is, we assume $D = dI, B = bI$ and $C = cI$, where I is the identity matrix. We denote the eigenvalues of matrix A by $\mu_1, \ldots, \mu_n$. Then the eigenvalues $z_1, \ldots, z_n$ of the smaller problem (17) are related to the μ_i by

$$\mu_i = z_i + d$$
$$z_i = \mu_i - d.$$

It follows from the equation (20) that the eigenvalues of Q satisfy $\det(A - uI) = 0$ where the constant

$$u = \frac{db + (d+b)\lambda + \lambda^2}{c}.$$

Therefore the eigenvalues come in pairs $\lambda_i^{\pm}$, where for each i they are related to eigenvalues $\mu_1, \ldots, \mu_n$ of A by

$$\mu_i = \frac{db + (d+b)\lambda_i + \lambda_i^2}{c}$$

or

$$\lambda_i^2 + \lambda_i(d+b) + db - \mu_i c = 0.$$

The solutions are

$$\lambda_i^{\pm} = \frac{1}{2}(-(d+b) \pm \sqrt{(d-b)^2 + 4\mu_i c}).$$

We note that the sets U and V described in the Theorem 3.3, can be obtained from the following two sets:

a. $W_1 := \{\mu \in \mathbb{C} \mid$ the real part of $z = \mu - d$ is negative$\}$,

b. $W_2 := \{\mu \in \mathbb{C} |$ the real part of at least one of $\lambda^{\pm} = \frac{1}{2}(-(d+b) + \sqrt{(d-b)^2 + 4\mu c})$ is positive. $\}$

Let $W := W_1 \cap W_2$ and $Z :=$ Int $(\bar{W}_1 \cap \bar{W}_2)$, where the bar denotes the complement of a set in the complex plane, and Int is the interior of a set. It follows that the set Z is the set of those μ where the real part of $z = \mu - d$ is positive and the real parts of both $\lambda^{\pm}$ are negative. With these definitions the sets

$$U = W - d, \quad \text{and } V = Z - d$$

are translations of the sets W and Z respectively.

The set W_1 has a very simple shape - it is a half-plane in a complex plane of the form $\Re e(\mu) < d$. We now investigate the set W_2. We first observe that

$$\Re e(\frac{1}{2}(-(d+b) \pm \sqrt{(d-b)^2 + 4\mu c})) > 0$$

is equivalent to

$$d + b < \pm \Re e(\sqrt{(d-b)^2 + 4\mu c}). \tag{21}$$

We write

$$\mu := re^{i\phi} \tag{22}$$

and set

$$ue^{i\theta} := (d-b)^2 + 4c\mu = (d-b)^2 + 4cre^{i\phi}. \tag{23}$$

Then the square root on the right hand side (21) has two solutions

$$w_1 = \sqrt{u}e^{i\theta/2} \quad \text{and} \quad w_2 = \sqrt{u}e^{i(\theta/2+\pi)}.$$

Taking the real part on the right hand side of the equation (21) we see that the inequality is equivalent to

$$d + b < \sqrt{u}\cos\theta/2 \quad \text{or} \quad d + b < \sqrt{u}\cos(\theta/2+\pi). \tag{24}$$

If we define the angle θ in (23) to be $-\pi \le \theta \le \pi$, then for $\theta/2$ we have $-\pi/2 \le \theta/2 \le \pi/2$. This implies that $\cos\theta/2 > 0$ and $\cos(\theta/2+\pi) < 0$ and the second inequality in (24) is never satisfied.

Therefore the region Y is bounded by the curve

$$\sqrt{u} > \frac{b+d}{\cos(\theta/2)}, \quad \text{where } -\frac{\pi}{2} \le \theta/2 \le \frac{\pi}{2}. \tag{25}$$

We now express this inequality in terms of u and θ, rather than $\sqrt{u}$ and $\theta/2$. Since $\cos\theta/2 \ge 0$ in the range of possible $\theta/2$, the inequality (25) is equivalent to $\cos^2(\theta/2) > \frac{(b+d)^2}{u}$. We multiply by 2, subtract 1 from both sides and use the double angle formula to get

$$\cos\theta > 2\frac{(b+d)^2}{u} - 1,$$

which yields

$$u > 2\frac{(b+d)^2}{1+\cos\theta}, \qquad -\pi < \theta < \pi \tag{26}$$

This formula has a clear geometric interpretation. As angle θ sweeps the range from $-\pi$ to π, the critical modulus

$$u^*(\theta) := 2\frac{(b+d)^2}{1+\cos\theta}$$

varies from $(b+d)^2$ at $\theta = 0$ (the positive real axis) to ∞ in the limit $\theta \to \pm\pi$ (the negative real axis). The function $u^*(\theta)$ in polar coordinates has apex at $(0, (b+d)^2)$ and is symmetric around the real axis since $u^*(\theta) = u^*(-\theta)$. The region $Y = \{ue^{i\theta} \in C \mid u > u^*(\theta)\}$ is the set of all complex numbers whose modulus is larger than $u^*(\theta)$.

From definition (23) we see that the set W_2 is a shifted and scaled version of the set Y. Indeed, the affine transformation $X := Y - (d-b)^2$ shifts the region Y to the left, but does not change the shape of Y. The coordinate of the apex of X on positive real axis will be

$$(b+d)^2 - (d-b)^2 = 4bd > 0.$$

Finally, a complex number $Re^{i\phi} \in X$ if, and only if, $4cre^{i\phi} \in W_2$. This means that $r = \frac{R}{4c}$ and the set W_2 can be obtained from the set X by dividing the radius along each ray by $4c$. The intersection of the set W_2 with the positive real axis is then

$$\{\mu \mid \mu > \frac{bd}{c}\}. \tag{27}$$

Now we turn to the sets $W = W_1 \cap W_2$ and $Z = \text{ Int } (\bar{W}_1 \cap \bar{W}_2)$, where Int denotes the interior of a set. Since W_1 is given by $\mu < d$ we see from (27) that if $b \geq c$, the intersection of W with the real axis is empty, while if $b < c$ this intersection is an interval $(\frac{b}{c}d, d)$. The set W is an unbounded subset of the set W_1 (see Figure 1). The set U is just a translation of the set W; if $b \geq c$ then U does not intersect the real axis, while if $b < c$, then this intersection is an open interval $((\frac{b}{c} - 1)d, 0)$.

The interior of the intersection $\bar{W}_1 \cap \bar{W}_2 = \emptyset$ when $b \leq c$, while when $b > c$ it is a bounded set around the positive real axis, intersecting this axis in the interval $(d, \frac{b}{c}d)$. The set V is just a translation of this intersection and intersects the positive real axis in the interval $(0, (\frac{b}{c} - 1)d)$.

5.2 Computer simulations

Numerical analysis was performed with custom software written in Python and C, using AUTO (`http://indy.cs.concordia.ca/auto/`) for dynamical continuation, and the CVODE module of Sundials (`https://computation.llnl.gov/casc/sundials/main.html`) for evaluation of particular time-series solutions. Source code is publicly available at `https://github.com/gic888/msu_rna_dynamics`), and is licensed under the GNU Public license (`http://www.gnu.org/copyleft/gpl.html`). Separate, but equivalent, specifications of both models (with and without explicit RNA) were implemented in C for use by Sundials, and FORTRAN for use by AUTO. Evaluation protocols and visualizations were written in Python.

We report results from two sorts of numerical investigations. The boundaries of the region of stable oscillations, in both of Figures 2 and 3, were computed by AUTO. The amplitudes of oscillation, as encoded by the colors in Figure 3 were computed from time-series evaluations of the system.

To compute the oscillation amplitude values, we sampled the reported range of the parameters α_2 and ϵ with a 100 by 100 grid of parameter values. For each point in this grid, we numerically integrated the model, using CVODE's BDF/Newton integrator, for 600 time units. We then discarded the first half of this time window, to remove the initial transients, and measured the peak-to-peak amplitude of the remaining time-series.

During the scans reported here, we used only a single initial condition (all state variables equal to 2). As a result, it is not surprising that in the interior of the fold, we sometimes do not detect oscillations even where a stable oscillatory state should exist according to the dynamics. It appears that, as α_2 increases and ϵ decreases, the oscillatory state becomes less and less numerically accessible. In additional scans using many sets of initial conditions, distributed in the vicinity of previously located oscillations, we were able to detect oscillations in more, but still not all, of this region. These explorations were computationally expensive, prone to numerical errors, and did not affect our conclusions about the overall system dynamics, and are therefore not reported here.

References

[1] M. Arcak and E. Sontag, (2006), Diagonal stability of a class of cyclic systems and its connection with the secant criterion, Automatica 42(9), 1531-1537.

[2] J. Collier, N. Monk, P. Maini and J. Lewis, (1996), Pattern formation by lateral inhibition with feedback: a mathematical model of Delta-Notch intercellular signaling, J. Theor. Biol 183, 429-446.

[3] M. B. Elowitz and S. Leibler,(2000), A synthetic oscillatory network of transcriptional regulators, Nature (London) 403, 335.

[4] J. Garcia-Ojalvo, M. B.Ellowitz and S. H.Strogatz, (2004), Modeling a synthetic multicellular clock: repressilators coupled by quorum sensing. PNAS. Vol.101. No.30, 10955-10960.

[5] *Cyclic feedback systems*, (1998), Memoirs of AMS, vol. 134, No. 637.

[6] T. Gedeon and K. Mischaikow, (1995), Structure of the global attractor of cyclic feedback systems, J. Dynam. Diff. Eq. 7, 141-190.

[7] T. Gedeon, K. Mischaikow, K. Patterson and E. Traldi, (2008), When activators repress and repressors activate: a qualitative analysis of Shea-Ackers model, Bulletin of Mathematical Biology, 70:6, 1660-1683.

[8] T. Gedeon, K. Mischaikow, K. Patterson and E. Traldi, (2008) Binding cooperativity in phage lambda is not sufficient to produce an effective switch, Biophysical J. 94(9), 3384-3393.

[9] B.C. Goodwin,(1965), Oscillatory behavior in enzymatic control processes. Adv Enzyme Regul. 3, 425-38.

[10] A. Kuznetsov, M. Kaern, and N. Kopell, (2004), Synchrony in a Population of Hysteresis-based Genetic Oscillators, SIAM J. Appl. Math. 65(2), 392-425.

[11] J. Lewis,(2003), Autoinhibition with Transcriptional Delay: A Simple Mechanism for the Zebrafish Somitogenesis Oscillator, Current Biology 13(16), 1398-1408.

[12] J. Mallet-Paret, (1988), Morse decompositions for delay differential equations, J. Diff. Eq. 72, 270-315.

[13] J. Mallet-Paret and H.L. Smith, (1990), The PoincarBendixson theorem for monotone cyclic feedback systems, J. Dyn. Diff. Eq. 2, 249-292.

[14] J. Mallet-Paret, G. R. Sell, (1996), The Poincar-Bendixson Theorem for Monotone Cyclic Feedback Systems with Delay, J. Diff. Eq. 125 (1996), 441489.

[15] D. McMillen, N. Kopell, J. Hasty, and J. Collins, (2002), Synchronizing genetic relaxation oscillators with intercell signaling, Proc. Natl. Acad. Sci. U.S.A. 99(2),679-684

[16] N. Monk, (2003), Oscillatory Expression of Hes1, p53, and NF-κ B Driven by Transcriptional Time Delays, Current Biology 13(16), 1409-1413.

[17] B. Novak, O. Kapuy, M.R. Domingo-Sananes, and J.J Tyson, (2010). Regulated protein kinases and phosphatases in cell cycle decisions. Curr. Opin. Cell Biol. 22:1-8.

[18] B. Novak and J.J. Tyson, (2008), Design principles of biochemical oscillators. Nature Rev. Mol. Cell Biol. 9:981-991.

[19] B. Novak and J.J. Tyson, (1993), Numerical analysis of a comprehensive model of M-phase control in Xenopus oocyte extracts and intact embryos. J. Cell Sci. 106, 11531168.

[20] J.R. Pomerening, E.D. Sontag and J.E. Ferrell Jr., (2003), Building a cell cycle oscillator: hysteresis and bistability in the activation of Cdc2, Nat. Cell Biol. 5, 346351.

[21] M. Shea and G. Ackers, (1985), The OR control system of bacteriophage lambda, a physical-chemical model for gene regulation, J. Mol. Biol. 181, 211-230.

[22] E. D. Sontag, (2006), Passivity gains and the secant condition for stability. Systems and Control Letters, 55, 177183.

[23] C.D. Thron, (1991), The secant condition for instability in biochemical feedback control-Parts I and II, Bulletin of Mathematical Biology, 53, 383-424.

[24] J.J. Tyson, H.G. Othmer, (1978), The dynamics of feedback control circuits in biochemical pathways. In R. Rosen, & F. M. Snell (Eds.), Progress in theoretical biology (Vol. 5, pp. 162). New York: Academic Press.

[25] Yang, Y., Kuznetsov, A., (2009), Characterization and merger of oscillatory mechanisms in an artificial genetic regulatory network, Chaos 19, 033115.